Analyst

PAPER

View Article Online
View Journal | View Issue

Cite this: *Analyst*, 2016, **141**, 4919

Visualization of exhaled hydrogen sulphide on test paper with an ultrasensitive and time-gated luminescent probe†

Ruilong Zhang,[a,b,c] Shijiang Liu,[a,b] Jianping Wang,[a] Guangmei Han,[a] Linlin Yang,[a,b] Bianhua Liu,*[a,c] Guijian Guan[a] and Zhongping Zhang*[a,b,c,d]

Received 10th April 2016,
Accepted 30th May 2016

DOI: 10.1039/c6an00830e

www.rsc.org/analyst

Luminescent chemosensors for hydrogen sulphide (H_2S) are of great interest because of the close association of H_2S with our health. However, current probes for H_2S detection have problems such as low sensitivity/selectivity, poor aqueous-solubility or interference from background fluorescence. This study reports an ultrasensitive and time-gated "switch on" probe for detection of H_2S, and its application in test paper for visualization of exhaled H_2S. The complex probe is synthesized with a luminescent Tb^{3+} centre and three ligands of azido ($-N_3$) substituted pyridine-2,6-dicarboxylic acid, giving the probe high hydrophilicity and relatively fast reaction dynamics with H_2S because there are three $-N_3$ groups in each molecule. The introduced $-N_3$ group as a strong electron-withdrawing moiety effectively changes the energy level of ligand *via* intramolecular charge transfer (ICT), and thus breaks the energy transferring from ligand to lanthanide ion, resulting in quenching of Tb^{3+} luminescence. On addition of H_2S, the $-N_3$ group can be reduced to an amine group to break the process of ICT, and the luminescence of Tb^{3+} is recovered at a nanomolar sensitivity level. With a long lifetime of luminescence of Tb^{3+} centre (1.9 ms), use of a time-gated technique effectively eliminates the background fluorescence by delaying fluorescence collection for 0.1 ms. The test paper imprinted by the complex probe ink can visualize clearly the trace H_2S gas exhaled by mice.

Introduction

Traditionally, hydrogen sulphide (H_2S) was considered to be a toxic gas with an unpleasant rotten egg smell, which could induce fatigue, headaches, and even probability of death in poorly ventilated environments.[1] Recently, however, it has been demonstrated that endogenous H_2S as the third gaseous signalling molecule has a role in numerous physiological processes.[2–5] Evidence has been provided[2–5] that endogenous H_2S is not only involved in a wide range of physiological processes such as relaxation of vascular smooth muscles and inhibition of insulin signaling,[2–4] but also maintains the redox equilibrium in living systems because of its strong reducibility to scavenge reactive oxygen/nitrogen species as well as its ability to regulate NO.[5] Abnormal levels of H_2S can induce various diseases, for instance, recent studies reported that H_2S concentrations of Parkinson's and Alzheimer's patients were relatively lower than those of healthy people.[6,7] Accordingly, there is a need for detection and quantification of H_2S in biological samples, to further understand its physiological functions.

Classical approaches to H_2S detection with high accuracy were electrochemical and chromatography analysis, which required complicated pretreatments of samples, professional operators and expensive spectrometers,[8,9] thus limiting their applications in fast and on-site assays of H_2S. To overcome these disadvantages, considerable efforts have been devoted to development of chemosensors for detection of H_2S, which most focused on a luminescent method with visualization and high sensitivity.[10,11] Selective reactions of luminescent probes with H_2S, including quencher ion (Cu^{2+}) removal,[12–15] nucleophilic and addition reactions with H_2S,[16–21] and reduction of the azido group ($-N_3$),[22–26] induce changes in luminescent signals, which reveal the presence and level of H_2S. The quencher ion removal and nucleophilic and addition reactions work on the

[a]*Center for Excellence in Nanoscience, Institute of Intelligent Machines, Chinese Academy of Sciences, Hefei, Anhui 230031, China. E-mail: bhliu@iim.ac.cn, zpzhang@iim.ac.cn*
[b]*Department of Chemistry, University of Science and Technology of China, Hefei, Anhui 230026, China*
[c]*School of Chemistry and Chemical Engineering, Anhui University, Hefei, 230601, China*
[d]*State Key Laboratory of Transducer Technology, Chinese Academy of Sciences, Hefei, Anhui 230031, China*

†Electronic supplementary information (ESI) available. See DOI: 10.1039/c6an00830e

basis of reaction activities of –SH, and thus thiols, such as cysteine (Cys) and glutathione (GSH) which are widely present in biological systems, could interfere with the detection. However, using $-N_3$ reduction, the recognized element can specifically respond to H_2S rather than thiols because H_2S have much stronger reducibility. Probes based on $-N_3$ reduction have several drawbacks, however, including low sensitivity, poor aqueous-solubility and slow dynamics.

Luminescent chemosensors have yet to overcome background fluorescences, which are widely existent in biological samples. Lanthanide emission centres have much longer luminescence lifetimes (at millisecond scale) than those of common organic dyes/quantum dots (at nanosecond scale).[27,28] Thus, a time-gated (or time-resolved) luminescence technique using a lanthanide ion probe is more suitable for detection of biological analytes. In addition, the emissions of lanthanide ions also have unique properties, such as sharp emission bands, large stocks shift and excellent photostability.[29] However, excitation of lanthanide ions is difficult because of the forbidden f–f transitions. Introducing one or more sensitizing chromophores as an antenna into the lanthanide complex can effectively transfer energy to lanthanide ions, resulting in strong emission of the lanthanide ions. In this study, a pyridine-2,6-dicarboxylic acid derivative is synthesized with an $-N_3$ group (DPA-N_3) as the antenna and ligand to prepare the probe $Na_3[Tb(DPA\text{-}N_3)_3]$. The three strong electron-withdrawing groups $-N_3$ not only induce the intramolecular charge transfer (ICT) to shut off the luminescence of the probe, but also provide three reactive sites specific to H_2S. On the addition of H_2S, the $-N_3$ groups are reduced and the strong green luminescence of Tb^{3+} is recovered. Additionally, the probe exhibits good solubility and fast dynamics in aqueous solution, and its unique applications in assays of H_2S are demonstrated, especially for visualization of H_2S exhaled by mice with test paper prepared using the probe.

Experimental section

Reagents and instruments

Chelidamic acid (DPA-OH), PCl_5, $Tb(NO_3)_3{\cdot}6H_2O$ and NaHS were purchased from Sigma. Other reagents were used as received from Shanghai Chemicals Ltd. ^1H and ^{13}C NMR spectra were performed on a Bruker Ultrashield spectrometer. Mass spectra (MS) were measured using an Agilent Q-TOF 6540 mass spectrometer. UV-visible absorption spectra were obtained with a Shimadu UV-2550 spectrometer. Elemental analyses were performed with a PerkinElmer 240C elemental analyzer. Luminescent spectra were recorded using a Cary Eclipse fluorescence spectrophotometer.

Synthesis of probe $Na_3[Tb(DPA\text{-}N_3)_3]$

Synthesis of 4-chloro-2,6-dimethylpyridinedicarboxylate (DPA-Cl methyl ester). DPA-OH (1.83 g, 10 mmol), PCl_5 (8.23 g, 40 mmol) and 30 mL $CHCl_3$ were put in a 100 mL flask and refluxed for 24 h. Then the solvent was distilled off and the residue was treated with 50 mL anhydrous CH_3OH in an ice-bath. The reaction mixture was stirred at 60 °C for 2 h. Excess CH_3OH was removed under reduced pressure. The solid was recrystallized in CH_3OH to obtain DPA-Cl methyl ester. ^1H NMR (400 MHz, $CDCl_3$, δ): 4.04 (s, 6H, $-CH_3$), 8.30 (s, 2H, -pyridine-H); MS (m/z, ESI) Calculated for $C_9H_8ClNO_4$ m/z = 229.01 [M + H]. Found m/z = 230.02.

Synthesis of 4-azido-pyridine-2,6-dicarboxylic acid (DPA-N_3). DPA-Cl methyl ester (0.11 g, 0.48 mmol), NaN_3 (0.16 g, 2.46 mmol) and 2 mL water were added to 8 mL DMF. After dissolving completely, the mixture was stirred at 80 °C for 12 h and the solvents were then removed under reduced pressure. The obtained solid was dissolved in NaOH aqueous solution (2%, 15 mL) and stirred at room temperature for 4 h. After the mixture was adjusted to neutral (pH 7) by HCl, the product DPA-N_3 was collected as a white solid in 55% yield. ^1H NMR (400 MHz, d_6-DMSO, δ): 7.86 (s, 2H, -pyridine-H); ^{13}C NMR (D_2O, δ):171.80, 154.49, 151.22, 115.18. MS (m/z, ESI) Calculated for $C_7H_4N_4O_4$ m/z = 208.02 [M − H]. Found m/z = 207.02.

Synthesis of $Na_3[Tb(DPA\text{-}N_3)_3]$. DPA-$N_3$ (0.21 g, 1.01 mmol) was dissolved in 15 mL H_2O, and the reaction mixture was adjusted to pH 7 by 0.1 M NaOH. Then $Tb(NO_3)_3{\cdot}6H_2O$ (0.15 g, 0.33 mmol) was added and stirred at room temperature for 4 h. After removing most of the water, 5 mL acetone was added in aqueous solution. The complex was given as a white solid. Anal. Calc. for $C_{21}H_6N_{12}Na_3O_{12}Tb$: C, 29.81; H, 0.71; N, 19.86 (%). Found: C, 29.80; H, 0.73; N, 19.84 (%). HR-MS (m/z, ESI) Calculated for $C_{21}H_6N_{12}Na_3O_{12}Tb$ m/z = 822.9277 [M − Na]. Found m/z = 799.9371.

Preparation of test paper and detection of exhaled H_2S

A common cartridge of a commercial inkjet printer was washed with ultrapure water until the ink was completely cleared away, and then the cartridge was dried. pH of the aqueous probe (1×10^{-4} M) was adjusted to 8.0 to facilitate absorption of acid H_2S gas, then 1 mL of aqueous probe was injected into the vacant cartridge. A square pattern (4×4 cm^2) was printed on a piece of paper by the printer under the control of computer. When the paper was dried, the paper was cut to 0.5×0.5 cm^2 for visualization of H_2S gas.

Male C57BL/6 mice (six weeks old, body weight = 50 ± 5 g) were injected with different dosages of NaHS aqueous solution (0.5, 1.0, 2.0 and 3.0 mg kg^{-1}). After 5 min, a treated mouse and a piece of wet test paper were simultaneously sealed into a 500 mL bottle for 45 min. During this process, the mice should be kept alive. Then, a photo of the reacted test paper was taken under a 254 nm UV lamp. Meanwhile, the amount of H_2S exhaled by the mice was also determined by a classical ion chromatography method to validate the reliability of the test paper. 10 mL of 1 M $(CH_3COO)_2Pb$ aqueous solution was placed on the bottom of each bottle to absorb H_2S exhaled by the mouse, and then refluxed with 1 M HNO_3 for 2 h to transform PbS into SO_4^{2-}. Finally, the concentration of SO_4^{2-} was determined by ion chromatography, and the amount of H_2S was calculated. The same experiments were repeated three times.

Results and discussion

Synthesis of probe $Na_3[Tb(DPA\text{-}NH_2)_3]$

Pyridine-2,6-dicarboxylic acid (DPA) is an excellent tridentate ligand to chelate Tb^{3+}, and can effectively transfer energy to Tb^{3+}, leading to generation of strong luminescence.[30] In this study, 4-hydroxyl substituted DPA (DPA-OH) was selected as the starting molecule, which could be reconstructed to modify the energy level of DPA and modulate the emission of its Tb^{3+} complex (Scheme 1). First, a phenol hydroxyl group and two carboxyl groups in DPA-OH were simultaneously chloridized with PCl_5, and the two formed acyl chlorides further reacted with methanol to form two methyl ester groups. Then, the $-N_3$ group was introduced by substituting the Cl atom of DPA-Cl methyl ester with NaN_3, and finally two methyl esters were hydrolyzed in NaOH solution at room temperature. The obtained ligand (DPA-N_3) was characterized by ^1H NMR, ^{13}C NMR, and MS (Fig. S1–S3†). The probe $Na_3[Tb(DPA\text{-}N_3)_3]$ was obtained by reaction of DPA-N_3 with $Tb(NO_3)_3{\cdot}6H_2O$ in aqueous solution. There were three $-N_3$ groups in each probe molecule to give the probe fast reaction dynamics with H_2S.

In the probe $Na_3[Tb(DPA\text{-}N_3)_3]$ molecule, the introduced $-N_3$ as a strong electron-withdrawing moiety can effectively change the energy level of ligand *via* ICT, which can break the energy transferring from ligand to Tb^{3+} and result in luminescence quenching of Tb^{3+} (Scheme 1). On addition of H_2S, following reduction of $-N_3$ to $-NH_2$, the process of ICT is prevented, and thus the energy transfer from ligand to Tb^{3+} is recovered, inducing luminescence of Tb^{3+}. To confirm the reaction mechanism of the luminescence response, the reaction of probe with H_2S was monitored by MS and fluorescent spectroscopy. Before addition of H_2S, the peak of $Na_2[Tb(DPA\text{-}N_3)_3]^-$ at m/z = 822.93 was clearly observed (Fig. 1A); meanwhile, the probe was almost nonluminescent (Fig. 1C). On addition of H_2S, the peak of probe at m/z = 822.93 disappeared and a new peak of reacted probe $Na_2[Tb(DPA\text{-}NH_2)_3]^-$ at m/z = 744.96 was detected (Fig. 1B). After reaction with H_2S, the probe exhibited strong emission with the four characteristic peaks of Tb^{3+} at 490 ($^5D_4$ to $^7F_6$), 545 ($^5D_4$ to $^7F_5$), 584 ($^5D_4$ to $^7F_4$) and 622 nm ($^5D_4$ to $^7F_3$) at excitation of 280 nm (Fig. 1C). Meanwhile, a bright green

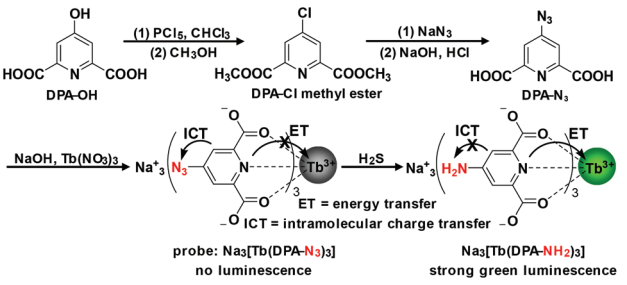

Scheme 1 Synthetic route of probe $Na_3[Tb(DPA\text{-}N_3)_3]$ and proposed reaction mechanism of $Na_3[Tb(DPA\text{-}N_3)_3]$ with H_2S.

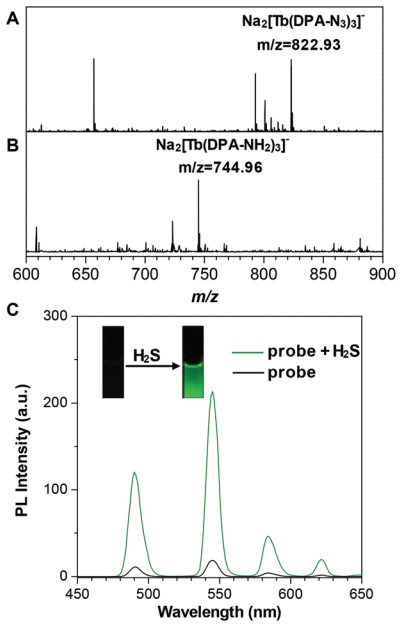

Fig. 1 (A, B) ESI-MS spectra (negative mode) of probe $Na_3[Tb(DPA\text{-}N_3)_3]$ and the mixture of $Na_3[Tb(DPA\text{-}N_3)_3]$ and H_2S. (C) Time-gated luminescent spectra of $Na_3[Tb(DPA\text{-}N_3)_3]$ before (black curve) and after (green curve) addition of H_2S at excitation of 280 nm. The delay time of time-gated spectra is 0.1 ms. The inset shows the corresponding photos under a 254 nm UV lamp.

luminescence was seen under a 254 nm UV lamp (Fig. 1C inset).

Time-gated luminescence response to H_2S

The luminescent lifetime of reacted probe $Na_3[Tb(DPA\text{-}NH_2)_3]$ was measured. As shown in Fig. 2A, using the time-gated technique, the luminescent lifetime at 545 nm was as long as 1.9 ms, sufficient to avoid interference from background fluorescences because of the lifetime of normal fluorescence at the nanosecond scale. The time-gated phosphorescent mode was set as listed in Table S1.† Fig. 2B shows the time-gated spectrum with delay time of collection set as 0.1 ms, and the steady-state fluorescent spectrum without delay time. The intensity of time-gated phosphorescence at 545 nm was 24.8-fold stronger than that of steady-state fluorescence, because most photons were counted in phosphorescence mode, with instantaneously produced photons only collected in fluorescence mode.[31] Meanwhile, the peak of second harmony generation (SHG) was completely eliminated using the time-gated technique. Significantly, the much stronger phosphorescence after the reaction of probe with H_2S suggests a much higher sensitivity of probe than that in normal fluorescent mode, when comparing the two mode spectra (Fig. 1C and S5†).

Fig. 3A shows the time-gated luminescent spectra of 3 μM $Na_3[Tb(DPA\text{-}N_3)_3]$ in the presence of different concentrations of H_2S. Here, NaHS was chosen as the source of H_2S and all the experiments were performed in HEPES buffer (pH 7.4).

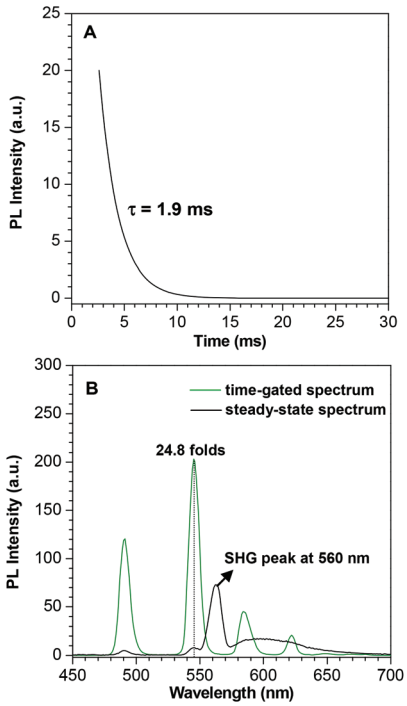

Fig. 2 (A) Luminescence decay of reacted probe $Na_3[Tb(DPA\text{-}NH_2)_3]$ (fit to a mono exponential function) monitoring at 545 nm in HEPES buffer (pH 7.4). (B) Time-gated (green curve) and steady-state (black curve) luminescent spectra of reacted probe $Na_3[Tb(DPA\text{-}NH_2)_3]$ at excitation of 280 nm. The delay time of time-gated spectra is 0.1 ms.

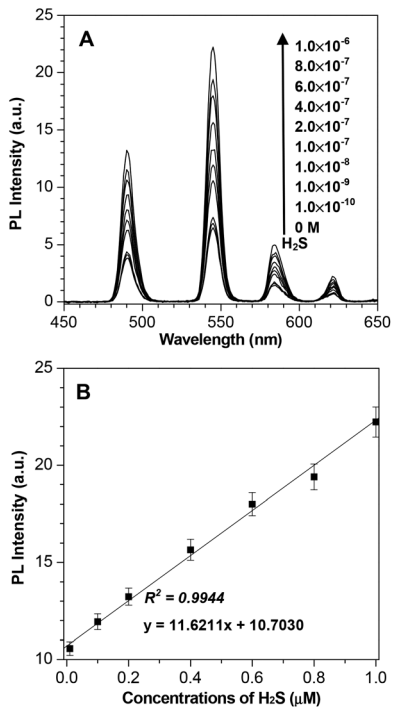

Fig. 3 (A) Time-gated luminescent spectra of $Na_3[Tb(DPA\text{-}N_3)_3]$ (3 μM) with addition of H_2S at excitation of 280 nm. The delay time of time-gated spectra is 0.1 ms. (B) Plots of luminescence enhancement at 545 nm *versus* H_2S concentrations.

Addition of H_2S caused the luminescence intensity of probe at 545 nm to increase continuously. When the concentration of H_2S reached 1 μM, approximately 3.2-fold luminescence enhancement was observed. Even at H_2S concentration as low as 0.1 nM, luminescence enhancement was enhanced by 5%, as observed clearly using the fluorescence spectrometer, suggesting the ultrasensitivity of the probe. As shown in Fig. 3B, luminescence enhancement at 545 nm was closely related to the dose of H_2S and displayed a good linearity with the H_2S concentrations in the range of 10 nM to 1 μM, with standard deviation R^2 = 0.9944. The results indicate that the probe can be used to quantify the amount of H_2S at the nanomolar level, satisfying the requirement of trace analysis.

To quantify the higher concentrations of H_2S, 50 μM probe $Na_3[Tb(DPA\text{-}N_3)_3]$ was used to perform the same test. It was found that the dose-dependent luminescence enhancement at 545 nm also showed a good linearity against the H_2S concentrations in the range of 1–100 μM, with standard deviation R^2 = 0.9960 (Fig. S6†). Meanwhile, the green luminescence could be seen clearly under the UV lamp (the inset in Fig. S6A†). Together with the above experimental results, it is indicated that the probe $Na_3[Tb(DPA\text{-}N_3)_3]$ can quantify amounts of H_2S in the very wide range of 10 nM–100 μM, by varying the amount of probe used.

Selectivity, dynamics and pH effect

In addition to H_2S, other species including various thiols, reactive oxygen species and anions are present in the biological samples. Therefore, it is essential to investigate the "turn-on" sensing selectivity of the probe for H_2S in buffer. Fig. 4A shows that H_2S with very low level (20 μM) induced dramatic enhancement of emission at 545 nm (11.2-fold), whereas 1 mM of other anions (HCO_3^-, F^-, Cl^-, Br^-, NO_3^-, $H_2PO_4^-$, citrate, SO_3^{2-}, $S_2O_3^{2-}$ and SO_4^{2-}) and reactive oxygen species (H_2O_2 and ClO^-) did not cause any significant luminescent response. In particular, the biological thiols, *e.g.* Cys, GSH and bovine serum albumin (BSA) did not cause any luminescent enhancement, confirming that $-N_3$ cannot be reduced by thiols in physiological conditions.[22–26] This sensing behaviour of the $Na_3[Tb(DPA\text{-}N_3)_3]$ probe indicates its high specificity to H_2S by the luminescence "turn-on" mechanism of $-N_3$ group reduction.

The dynamics of luminescence response of probe to H_2S also were examined by the time-dependent luminescence intensities of probe in the presence of H_2S at room temperature (Fig. 4B). The luminescence intensity at 545 nm increased to the maximum peak in about 20 min and remained unchanged as the reaction time was prolonged to 60 min, suggesting the probe has relatively fast dynamics even at only 1 μM H_2S. This is mainly because the probe has good aqueous-solubility and contains three $-N_3$ groups in each molecule.

Moreover, the effect of pH value was evaluated on luminescence response to confirm the pH range of probe used. Obvious luminescence enhancements of probe were observed in the presence of H_2S in a pH range of 6–10 (Fig. S7†), indicat-

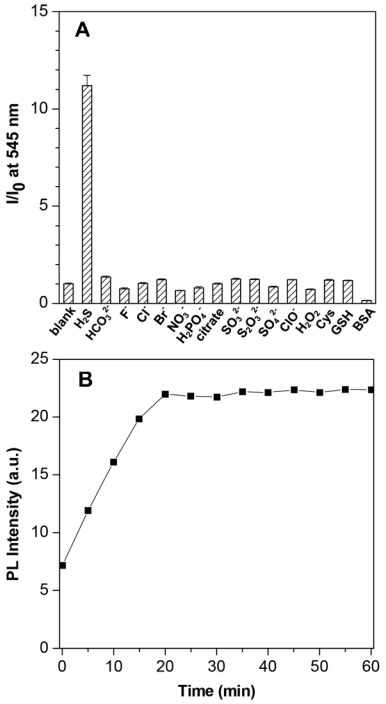

Fig. 4 (A) Luminescence enhancement (I/I_0) of $Na_3[Tb(DPA\text{-}N_3)_3]$ (3 μM in pH 7.4 HEPES buffer) in the presence of H_2S, various anions and biologically relevant species. The concentration of H_2S used was 20 μM, and HCO_3^-, F^-, Cl^-, Br^-, NO_3^-, $H_2PO_4^-$, citrate, SO_3^{2-}, $S_2O_3^{2-}$, SO_4^{2-}, H_2O_2, ClO^-, cysteine (Cys), glutathione (GSH) and bovine serum albumin (BSA) were 1 mM. (B) Time-dependent luminescence intensities of $Na_3[Tb(DPA\text{-}N_3)_3]$ (3 μM) at 545 nm in the presence of 1 μM H_2S for 60 min at room temperature.

ing that the probe can be used to detect H_2S in biological samples, such as blood plasma.

Practical applications in blood plasma

To certify that the probe $Na_3[Tb(DPA\text{-}N_3)_3]$ can be used in biological samples, 20 μL of fresh plasma sample from healthy volunteers were added to 1.98 mL of 3 μM $Na_3[Tb(DPA\text{-}N_3)_3]$ aqueous solution (total volume was 2 mL). The concentration of H_2S in plasma was determined to be about 31 μM, consistent with the value from ion chromatography (33.4 μM). Known amounts of H_2S were spiked into the plasma, with the results summarized in Table 1. The recoveries suggest that the probe $Na_3[Tb(DPA\text{-}N_3)_3]$ is reliable for the detection of H_2S and possesses potential for practical applications.

Table 1 Application of the probe $Na_3[Tb(DPA\text{-}N_3)_3]$ in determination of H_2S in fresh blood plasma. Recovery (100%) = (measured value/actual value) × 100%

Spiked (μM)	Found (μM)	Recovery (%)
0	31.4	94.6 ± 2.1
10	42.2	97.7 ± 2.7
20	53.5	100.4 ± 3.4
30	62.3	99.4 ± 2.5

Here, the volumes of samples used were only 20 μL because of the ultrasensitivity of probe $Na_3[Tb(DPA\text{-}N_3)_3]$, which could further suppress the background fluorescence of samples by dilution of 100-fold. Moreover, comparison of time-gated with steady-state spectra of pure plasma showed that no phosphorescence signal was detected in the time-gated spectrum (Fig. S8†), while the background fluorescences in the steady-state spectrum were superstrong. The results suggest that the background fluorescences were completely eliminated in practical biological samples using the time-gated technique.

Paper-based sensor for visual detection of exhaled H_2S

The amount of exhaled H_2S depends strongly on the concentration of H_2S in body liquid, so the level of exhaled H_2S can be used to evaluate individual health.[32] However, a simple, cheap and reliable method for visual detection of exhaled H_2S does not yet exist. A H_2S-responsive paper sensor was developed for visual detection of H_2S. The test paper was prepared by imprinting probe aqueous solution (1×10^{-4} M, pH 8.0) onto a piece of filter paper using an inkjet-printer connected with a computer (as described in the Experimental section).[33]

Before detection of bio-originating H_2S gas, the visual detection of H_2S in atmosphere on the test paper was investigated (Fig. 5A). Under a 254 nm UV lamp, the paper sensors emitted only weak blue fluorescence generated from the filter paper itself. With increasing amounts of H_2S, the test papers showed discernable changes of colour and brightness under a UV lamp. Even at 1 ppm H_2S, the test paper displayed a cyan colour, resulting from the mixture of the green emission of Tb^{3+} and the blue emission of filter paper. When the concentrations of H_2S were 10, 20 and 30 ppm in atmosphere, the test paper became grey, bright green and yellow-green, respectively, demonstrating visualization of H_2S in the atmosphere. The images in Fig. 5A can be taken as the standard cards for semi-quantification of gaseous H_2S.

Furthermore, attempts were made to measure the H_2S exhaled by mice using the test paper. To increase the amount of exhaled H_2S, different dosages of NaHS were injected into the enterocoelia of mice (Fig. 5B).[34] After 5 min, the treated

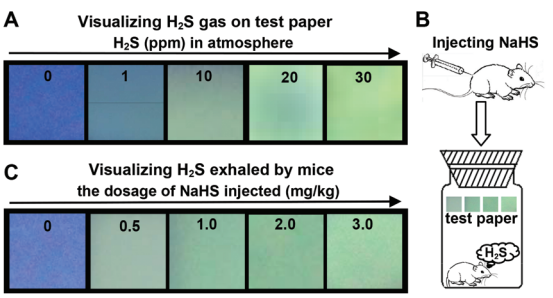

Fig. 5 (A) Paper-based visual detections of H_2S gas at different concentrations of 0, 10, 20 and 30 ppm. (B) Illustration of experimental procedures for the visualization of H_2S exhaled by mice. (C) Visualization of H_2S exhaled by mice using the test paper. The luminescence images of test paper were obtained under a 254 nm UV lamp. The size of test paper was 0.5 × 0.5 cm^2.

mice and a piece of test paper were simultaneously sealed in a bottle for 45 min (see the Experimental section). Fig. 5C shows the visualization of H_2S exhaled by mice treated with different dosages of NaHS. Even the exhaled gas from a normal state mouse without injection of NaHS, could induce the test paper to become brighter in comparison with the atmosphere without H_2S. That is to say, the test paper can produce a visual luminescence response to the H_2S exhaled by a normal state mouse. When 0.5 or 1.0 mg kg^{-1} NaHS were injected into the enterocoelia of mouse, the test paper exhibited grey and light green, respectively. In the case of 2.0 or 3.0 mg kg^{-1} NaHS, the test paper showed almost the same colour of green, and became brighter than that of 1 mg kg^{-1} NaHS. This indicates that the amounts of H_2S were highly correlated with the dosage of NaHS injected, and that the enhancement effect was much weaker when the injected NaHS was higher than 2 mg mL^{-1}. It should be noted that higher amounts of NaHS will cause the death of mice.

Compared with the results in Fig. 5A, the amount of H_2S exhaled by a mouse injected with 0.5 mg kg^{-1} NaHS was about 10 ppm, and 1.0, 2.0 or 3.0 mg kg^{-1} NaHS could induce mice to exhale about 10–20 ppm H_2S gas. To certify the reliability of the as-prepared test paper, exhaled H_2S also was determined using a traditional method by absorption of $(CH_3COO)_2Pb$ (see the Experimental section). After the mice were injected with 0.5, 1.0, 2.0 or 3.0 mg kg^{-1} NaHS, the amounts of exhaled H_2S were measured as 9.1 ± 0.6, 15.3 ± 0.7, 18.4 ± 1.1 or 20.4 ± 0.9 ppm, respectively, in accordance with measurements made using the test papers.

Conclusions

In summary, a Tb^{3+}-centred ultrasensitive luminescent probe was synthesized based on the reaction of $-N_3$ with H_2S, and achieved detection of trace H_2S in biological samples using a time-gated technique. The probe can react with H_2S and produce strong green luminescence, exhibiting three remarkable features: (1) long lifetime; (2) good aqueous-solubility and ultrasensibility; (3) wide linear range (10 nM–100 μM) and relatively fast luminescent response. On the basis of the above advantages, the probe not only effectively eliminates the background fluorescence of biological sample by fluorescence collection delayed for 0.1 ms, but also can be used to accurately quantify the level of H_2S in blood plasma. H_2S test paper was prepared using the Tb^{3+}-centred probe and its applications were demonstrated in detection of H_2S gas in the atmosphere and that exhaled by mice. The results reported here suggest that such a Tb^{3+}-centred probe could be a powerful tool in investigations of H_2S in complicated biological samples and exhaled gas.

Acknowledgements

This work was supported by the National Basic Research Program of China (2015CB932002), China-Singapore Joint Project (2015DFG92510), Science and Technology Service Network Initiative of Chinese Academy of China (KFJ-SW-STS-172), National Natural Science Foundation of China (21335006, 21475135, 21375131, 21277145) and Natural Science Foundation of Anhui Province (1408085MKL52, 1508085SQB200).

Notes and references

1 K. Hemminki and M. L. Niemi, *Int. Arch. Occup. Environ. Health*, 1982, **51**, 55–63.
2 G. Yang, L. Wu, B. Jiang, W. Yang, J. Qi, K. Cao, Q. Meng, A. K. Mustafa, W. Mu, S. Zhang, S. H. Snyder and R. Wang, *Science*, 2008, **322**, 587–590.
3 Y. Kaneko, Y. Kimura, H. Kimura and I. Niki, *Diabetes*, 2006, **55**, 1391–1397.
4 W. Yang, G. Yang, X. M. Jia, L. Wu and R. Wang, *J. Physiol.*, 2005, **569**, 519–531.
5 N. J. Alp and K. M. Channon, *Arterioscler., Thromb., Vasc. Biol.*, 2004, **24**, 413–420.
6 K. Eto, T. Asada, K. Arima, T. Makifuchi and H. Kimura, *Biochem. Biophys. Res. Commun.*, 2002, **293**, 1485–1488.
7 X. Xue and J. S. Bian, *Methods Enzymol.*, 2015, **554**, 169–186.
8 V. Kuban, P. K. Dasgupta and J. N. Marx, *Anal. Chem.*, 1992, **64**, 36–43.
9 D. M. Tsai, A. S. Kumar and J. M. Zen, *Anal. Chim. Acta*, 2006, **556**, 145–150.
10 X. Li, X. Gao, W. Shi and H. Ma, *Chem. Rev.*, 2014, **114**, 590–659.
11 X. Chen, X. Tian, I. Shin and J. Yoon, *Chem. Soc. Rev.*, 2011, **40**, 4783–4804.
12 K. Sasakura, K. Hanaoka, N. Shibuya, Y. Mikami, Y. Kimura, T. Komatsu, T. Ueno, T. Terai, H. Kimura and T. Nagano, *J. Am. Chem. Soc.*, 2011, **133**, 18003–18005.
13 C. Kar, M. D. Adhikari, A. Ramesh and G. Das, *Inorg. Chem.*, 2013, **52**, 743–752.
14 Y. Ma, H. Su, X. Kuang, X. Li, T. Zhang and B. Tang, *Anal. Chem.*, 2014, **86**, 11459–11463.
15 M. G. Choi, S. Cha, H. Lee, H. L. Jeon and S. K. Chang, *Chem. Commun.*, 2009, **45**, 7390–7392.
16 Y. Chen, C. Zhu, Z. Yang, J. Chen, Y. He, Y. Jiao, W. He, L. Qiu, J. Cen and Z. Guo, *Angew. Chem., Int. Ed.*, 2013, **52**, 1688–1691.
17 C. R. Liu, B. Peng, S. Li, C. M. Park, A. R. Whorton and M. Xian, *Org. Lett.*, 2012, **14**, 2184–2187.
18 C. R. Liu, J. Pan, S. Li, Y. Zhao, L. Y. Wu, C. E. Berkman, A. R. Whorton and M. Xian, *Angew. Chem., Int. Ed.*, 2011, **50**, 10327–10329.
19 E. Karakuş, M. Üçüncü and M. Emrullahoğlu, *Anal. Chem.*, 2015, **88**, 1039–1043.
20 D. Maity, A. Raj, P. K. Samanta, D. Karthigeyan, T. K. Kundu, S. K. Pati and T. Govindaraju, *RSC Adv.*, 2014, **4**, 11147–11151.

21 Y. Qian, J. Karpus, O. Kabil, S. Y. Zhang, H. L. Zhu, R. Banerjee, J. Zhao and C. He, *Nat. Commun.*, 2011, **2**, 495.
22 H. Peng, Y. Cheng, C. Dai, A. L. King, B. L. Predmore, D. J. Lefer and B. Wang, *Angew. Chem., Int. Ed.*, 2011, **50**, 9672–9675.
23 S. Chen, Z. Chen, W. Ren and H. Ai, *J. Am. Chem. Soc.*, 2012, **134**, 9589–9592.
24 A. R. Lippert, E. J. New and C. J. Chang, *J. Am. Chem. Soc.*, 2011, **133**, 10078–10080.
25 T. S. Bailey and M. D. Pluth, *J. Am. Chem. Soc.*, 2013, **135**, 16697–16704.
26 M. K. Thorson, T. Majtan, J. P. Kraus and A. M. Barrios, *Angew. Chem., Int. Ed.*, 2013, **52**, 4641–4644.
27 Z. Dai, L. Tian, B. Song, Z. Ye, X. Liu and J. Yuan, *Anal. Chem.*, 2014, **86**, 11883–11889.
28 G. Cui, Z. Ye, J. Chen, G. Wang and J. Yuan, *Talanta*, 2011, **84**, 971–976.
29 J. C. G. Bunzli, *Chem. Rev.*, 2010, **110**, 2729–2755.
30 J. B. Lamture, Z. H. Zhou, A. S. Kumar and T. G. Wensel, *Inorg. Chem.*, 1995, **34**, 864–869.
31 D. C. Lamb, A. Schenk, C. Röcker, C. Scalfi-Happ and G. U. Nienhaus, *Biophys. J.*, 2000, **79**, 1129–1138.
32 S. C. Sturney, M. K. Storer, G. M. Shaw, D. E. Shaw and M. J. Epton, *Thorax*, 2013, **68**, A141–A142.
33 Q. Mei and Z. Zhang, *Angew. Chem., Int. Ed.*, 2012, **51**, 5602–5606.
34 C. F. Toombs, M. A. Insko, E. A. Wintner, T. L. Deckwerth, H. Usansky, K. Jamil, B. Goldstein, M. Cooreman and C. Szabo, *Br. J. Clin. Pharmacol.*, 2010, **69**, 626–636.